

**ENHANCEMENT OF PRODUCER GAS QUALITY  
THROUGH CO<sub>2</sub> ABSORPTION USING CaO-SAND  
MIXTURE IN A FLUIDIZED BED REACTOR**

**MOHD MAHADZIR BIN MOHAMMUD @ MAHMOOD**

**UNIVERSITI SAINS MALAYSIA  
2012**

**ENHANCEMENT OF PRODUCER GAS QUALITY THROUGH CO<sub>2</sub>  
ABSORPTION USING CaO-SAND MIXTURE IN A FLUIDIZED  
BED REACTOR**

**by**

**MOHD MAHADZIR BIN MOHAMMUD @ MAHMOOD**

**Thesis submitted in fulfillment of the  
requirements for the degree of  
Doctor of Philosophy**

**December 2012**

## ACKNOWLEDGEMENT

Bismillahirrahmanirahim, Alhamdulillah, I would like to start by giving my thanks to Allah S.W.T Almighty for giving me the strength and inspiration to complete my Ph.D dissertation. I also would like to extend a very special thanks to my mum, father, brothers, beloved wife (Rozialina binti Mat Zain) and my children's (Muhammad Mifzal, Rusydina Madihah and Muhammad Mirza) for all their patience and understanding. Without their support, this dissertation will never be completed.

Thanks are also due to the research supervisor, Professor Dr. Hj. Zainal Alimuddin bin Zainal Alauddin from the USM School of Mechanical Engineering who gave a lot of guidance, counsel and recommendations of this study. Without knowledge and experience, this study may not be successfully completed.

In addition, appreciation is also given to all my friends especially Mr. Zalmi for their help. Last but not least thanks to the Universiti Teknologi MARA (UiTM), for provided the scholarships during my study. Without it, education and research may not be carried out completely. Moreover, I would like to thank all those involved directly or indirectly to the success of this research study.

Mohd Mahadzir bin Mohammad @ Mahmood

## TABLE OF CONTENTS

Acknowledgements .....	ii
Table of Contents .....	iii
List of Tables .....	viii
List of Figures .....	x
List of Abbreviations .....	xvi
List of Symbols .....	xvii
Abstrak .....	xxi
Abstract .....	xxiv

### CHAPTER ONE : INTRODUCTION

1.1 Fuel Scenario in Malaysia .....	1
1.2 Biomass . .....	3
1.3 Carbon Dioxide Capture .....	6
1.4 Problem Statements .....	9
1.5 Research Objectives .....	11
1.6 Research Scope .....	12
1.7 Organization Chapters .....	12

### CHAPTER TWO : LITERATURE REVIEW

2.1 Introduction.....	14
2.2 Biomass Gasification.....	14
2.2.1 Types of gasifier.....	15
2.2.2 Fixed bed gasifier.....	15

2.2.3	Fluidized bed gasifier.....	17
2.2.4	Wood Gasification.....	19
2.2.5	Producer Gas Composition from a Downdraft Gasifier...	21
2.2.6	Producer Gas Energy Content.....	24
2.3	Methods to Increase Producer Gas Quality.....	26
2.4	Carbon Dioxide (CO <sub>2</sub> ) Sorbent.....	32
2.4.1	Calcium Oxide (CaO).....	33
2.4.2	Absorption/Desorption Kinetic Reactions.....	33
2.4.3	Sorbent Reactivity over Multicyclic Reactions.....	39
2.5	CFD Modeling on Bubbling Fluidized Bed.....	46
2.5.1	Eulerian-Eulerian (Two-Fluid) Model Concept .....	50
2.5.2	Multiphase Granular Flow Theory.....	50
2.5.2.1	Continuity Equation.....	51
2.5.2.2	Momentum Equation.....	52
2.5.2.3	Granular Temperature.....	53
2.5.3	Theory of Hydrodynamic Properties.....	54
2.5.3.1	Granular Viscosity.....	54
2.5.3.2	Granular Bulk Viscosity.....	55
2.5.3.3	Granular Conductivity.....	55
2.5.4	Interaction: Momentum Transfer between Phases.....	56
2.5.4.1	Gidaspow Drag Model.....	56
2.5.4.2	Syamlal-O' Brien Drag Model.....	57
2.5.4.3	Wen-Yu Drag Model.....	58
2.6	Summary of Literature Review.....	59

**CHAPTER THREE : DESIGN AND DEVELOPMENT OF  
BUBBLING FLUIDIZED BED CO<sub>2</sub>  
ABSORPTION REACTOR**

3.1	Introduction.....	61
3.2	Bubbling Fluidized Bed Concept.....	61

3.3	Bed Particles.....	63
3.4	Estimation of Design Parameters.....	64
3.5	CO <sub>2</sub> BFBAR.....	69
3.6	CO <sub>2</sub> BFBAR Operating Parameters.....	70
	3.6.1 Aspect Ratio.....	70
	3.6.2 Pressure Drop.....	71
	3.6.3 Minimum Fluidization Velocity.....	72
	3.6.4 Terminal Velocity.....	75
	3.6.5 Volume Flow Rate.....	77
3.7	Gas Distributor.....	80

## CHAPTER FOUR : METHODOLOGY

4.1	Introduction.....	85
4.2	Characteristics of Furniture Wood.....	86
	4.2.1 Moisture Content Test.....	87
	4.2.2 Bomb Calorimeter Test.....	88
4.3	Numerical Approach and Simulation Setup.....	89
	4.3.1 Grid Generation.....	90
	4.3.2 Steps for Using Eulerian Multiphase Model.....	92
	4.3.2.1 Defining the Phases.....	92
	4.3.2.2 Boundary Conditions.....	93
	4.3.2.3 Initialization.....	94
	4.3.2.4 Stability and Convergence.....	95
	4.3.2.5 Post-processing.....	96
	4.3.3 Grid Independence Analysis .....	98
4.4	Statistical Analysis .....	101
4.5	Instrument and Measurement.....	103
	4.5.1 Ceramic Band Heater and Controller.....	103
	4.5.2 Data Acquisition.....	104
	4.5.3 Gas Chromatograph.....	105
	4.5.4 Gas Sampling Train.....	106

4.6	Downdraft Gasifier Experiment.....	107
4.6.1	Flare Test of Producer Gas.....	110
4.7	Characteristics of CO <sub>2</sub> BFBAR.....	112
4.7.1	Cold Model Experiment.....	112
4.7.2	Materials and Methods.....	114
4.7.3	CO <sub>2</sub> Absorption Experiment (Hot Model) .....	116
4.7.3.1	Simulated Gas (SG).....	116
4.7.3.2	Simulated Producer Gas (SPG).....	119
4.7.3.3	Compressed Producer Gas (CPG).....	119
4.7.4	Absorption-Desorption Experiment using TGA.....	121

## CHAPTER FIVE : RESULTS AND DISCUSSIONS

5.1	Introduction.....	124
5.2	Characteristics of Furniture Wood.....	124
5.2.1	Moisture Content Test.....	124
5.2.2	Bomb Calorimeter Test.....	125
5.3	FLUENT Simulation.....	126
5.4	Statistical Analysis.....	132
5.5	Cold Model Experiment.....	134
5.5.1	Effect of CaO-Sand Mixture Ratio to the Height of Bed Expansion.....	135
5.5.2	The Effect of CaO Particle Size to the Height of Bed Expansion.....	139
5.5.3	The Effect of Air Volume Flow Rate and Pressure to the Height of Bed Expansion.....	140
5.5.4	Volumetric Flow Rate Effects on the Mass of CaO in CO <sub>2</sub> BFBAR.....	143
5.6	Pressure Drop in CO <sub>2</sub> BFBAR.....	148
5.7	Absorption – Desorption Experiment with TGA.....	152
5.8	CO <sub>2</sub> Absorption Experiment with Simulated Gas (SG).....	159
5.9	CO <sub>2</sub> Absorption Experiment with Simulated Producer Gas.....	162

5.10	Downdraft Gasification Experiment.....	167
5.11	CO <sub>2</sub> Absorption Experiment with Compressed Producer Gas...	168

## **CHAPTER SIX : CONCLUSION**

6.1	Hydrodynamic Simulation.....	172
6.2	Design and Development of CO <sub>2</sub> BFBAR.....	173
6.3	Experiments.....	174
6.4	Recommendations for Future Research.....	176

<b>REFERENCES</b>		<b>178</b>
-------------------	--	------------

## **APPENDICES**

Appendix A - Drawing of CO <sub>2</sub> BFBAR.....	197
Appendix B – CFD (Fluent) Procedure .....	207
Appendix C - Moisture Content Test.....	214
Appendix D - Bomb Calorimeter Test Procedure.....	216
Appendix E - Fluent Simulation (Hydrodynamic Expansion).....	220
Appendix F - Raw Data of Cold Model Experiment.....	227
Appendix G – TGA Experimental Methods.....	239
Appendix H - List of Publications.....	241



## LIST OF TABLES

<b>Table 2.1:</b> Gas composition in the producer gas reported by other researchers using downdraft gasifier.	24
<b>Table 2.2:</b> Comparison of heating values of the producer gas obtained by other researchers	25
<b>Table 3.1:</b> The detail of Geldart groups for each solid particle	63
<b>Table 3.2:</b> Design parameters for 1 hour experiment	68
<b>Table 3.3:</b> Design parameters of CO <sub>2</sub> BFBAR	74
<b>Table 3.4:</b> Operating parameters of CO <sub>2</sub> BFBAR for absorption process with simulated gas ( $\text{CaO} + \text{CO}_2 \rightarrow \text{CaCO}_3$ )	78
<b>Table 3.5:</b> Operating parameters of CO <sub>2</sub> BFBAR for absorption process with producer gas ( $\text{CaO} + \text{CO}_2 \rightarrow \text{CaCO}_3$ )	79
<b>Table 3.6:</b> Operating parameters of CO <sub>2</sub> BFBAR for desorption process with air ( $\text{CaCO}_3 \rightarrow \text{CaO} + \text{CO}_2$ )	79
<b>Table 3.7:</b> Operating parameters of CO <sub>2</sub> BFBAR for cold model experiment using air	80
<b>Table 3.8:</b> Estimation of Fluidizing Condition	81
<b>Table 4.1:</b> Computational model parameters (50% CaO-sand mixture)	98
<b>Table 4.2:</b> Grid independence analysis	99
<b>Table 4.3:</b> Specification of gasifier	108
<b>Table 4.4:</b> CaO weight for 4 cm height	114
<b>Table 5.1:</b> The frequency data of bed expansion height	133
<b>Table 5.2:</b> Results analysis “SPSS Statistics 17”	134
<b>Table 5.3:</b> CaO-sand mixture data	135

<b>Table 5.4:</b> Expected minimum fluidization velocity	149
<b>Table 5.5:</b> SPG composition before and after CO <sub>2</sub> BFBAR	164
<b>Table 5.6:</b> LHV of SPG before and after CO <sub>2</sub> BFBAR	165
<b>Table 5.7:</b> Composition and Low Heating Value of CPG	167
<b>Table 5.8:</b> CPG composition and LHV after CO <sub>2</sub> BFBAR	170

## LIST OF FIGURES

<b>Figure 1.1</b> : Malaysia oil reserves (Top), Malaysia oil production and consumption (below)	2
<b>Figure 1.2</b> : The thermochemical processes and products.	5
<b>Figure 2.1</b> : Diagram of a downdraft gasifier	16
<b>Figure 2.2</b> : Diagram of an updraft gasifier	16
<b>Figure 2.3</b> : Diagram of a cross flow gasifier	17
<b>Figure 2.4</b> : Diagram of a) bubbling bed. b) circulating bed	19
<b>Figure 2.5</b> : $P_{CO_2,eq}$ over CaO as function of temperature.	34
<b>Figure 2.6</b> : A cycle of CO <sub>2</sub> absorption and desorption observed by TGA.	37
<b>Figure 2.7</b> : First desorption/absorption cycle for 250-425 micron Havelock limestone desorption 850°C with N <sub>2</sub> and absorbed at 580°C with 8% CO <sub>2</sub> , 21% H <sub>2</sub> , 42% CO, and 12% N <sub>2</sub> .	38
<b>Figure 2.8</b> : Cyclic desorption/absorption for 250-425 micron Havelock limestone desorption 850°C with N <sub>2</sub> and absorbed at 620°C with 8% CO <sub>2</sub> , 21% H <sub>2</sub> , 42% CO, and 12% N <sub>2</sub> .	39
<b>Figure 2.9</b> : CO <sub>2</sub> -Sorbent performance of CaCO <sub>3</sub> from different authors.	41
<b>Figure 2.10</b> : Conversion curves vs. time for different cycle numbers. Limestone Piaseck: dp 0.4-0.6 mm, temperature absorption 650°C for 5 min.	41
<b>Figure 2.11</b> : Conversion curve vs. time for different particle size. Limestone: La Blance, CO <sub>2</sub> particle pressure 0.01MPa, $T_{absorption}$ 650°C for 20 min, $T_{desorption}$ 850°C for 15 min. Left: cycle 1, Right: Cycle 20.	43

<b>Figure 2.12:</b> Conversion curves vs. time for different CO <sub>2</sub> partial pressure. Limestone: La Blance, dp: 0.4-0.6mm, $T_{\text{absorption}}$ 650oC for 20 min, $T_{\text{desorption}}$ 900oC for 15 min. Left: cycle 1, Right: Cycle 10, Below: cycle 40	44
<b>Figure 2.13:</b> Conversion curves vs. time for different $T_{\text{absorption}}$ . Limestone: La Blance, dp: 0.4-0.6mm, $T_{\text{desorption}}$ 900°C for 15 min. Left: cycle 40, Right: Cycle 150.	45
<b>Figure 3.1 :</b> Drawing of the CO <sub>2</sub> BFBAR	69
<b>Figure 3.2 :</b> Relation between pressure drop, bed height and superficial velocity.	71
<b>Figure 3.3 :</b> A nozzle type tuyere gas distributor plate	84
<b>Figure 4.1 :</b> Types of the experimental work	85
<b>Figure 4.2 :</b> Flow process to characterize the wood	86
<b>Figure 4.3 :</b> The Infrared Moisture Balance Machine	87
<b>Figure 4.4 :</b> A small block of wood	88
<b>Figure 4.5 :</b> Bomb Calorimeter	89
<b>Figure 4.6a:</b> Illustration of the boundary conditions CO <sub>2</sub> BFBAR 3-D	90
<b>Figure 4.6b:</b> Illustration of the velocity inlet boundary conditions CO <sub>2</sub> BFBAR 3-D	91
<b>Figure 4.7 :</b> The transparent CO <sub>2</sub> BFBAR	91
<b>Figure 4.8 :</b> The flow process of the simulation	97
<b>Figure 4.9a:</b> Pressure contours of CO <sub>2</sub> -sand mixture (a) Mesh size 6 mm (b) Mesh size 4 mm (c) Mesh size 2 mm	100
<b>Figure 4.9b:</b> Contour of CO <sub>2</sub> -sand mixture volume fraction (U = 0.214 m/s, t = 20 s): (a) Mesh size 6 mm (b) Mesh size 4 mm (c) Mesh size 2 mm	101

<b>Figure 4.10:</b> Ceramic band heater and controller	103
<b>Figure 4.11:</b> Ceramic band heater produced heat energy	104
<b>Figure 4.12:</b> DIGI-SENSE scanning Thermometer	104
<b>Figure 4.13:</b> Gas Chromatograph	105
<b>Figure 4.14:</b> Gas sampling train	106
<b>Figure 4.15:</b> The Tedlar sampling bags	107
<b>Figure 4.16:</b> Downdraft Gasifier System	109
<b>Figure 4.17:</b> Schematic diagram of downdraft gasifier system expansion height (500 micron and 70% CaO mixture)	109
<b>Figure 4.18:</b> Different flare test visualization of producer gas	111
<b>Figure 4.19:</b> Photograph of cold model experiment apparatus	112
<b>Figure 4.20:</b> Diagram of CO <sub>2</sub> BFBAR	113
<b>Figure 4.21:</b> Schematic diagram of cold model experiment set-up.	113
<b>Figure 4.22:</b> Photograph of 100, 500 and 1000 micron particle sizes of CaO	115
<b>Figure 4.23:</b> Photograph of hot model experiment apparatus with simulated gas	117
<b>Figure 4.24:</b> Schematic diagram of hot model experiment set-up. 1-4 refer to thermocouples used	117
<b>Figure 4.25:</b> An Endecott's multi-layer test sieve shaker	118
<b>Figure 4.26:</b> CPG experiment affiliated with CO <sub>2</sub> BFBAR	120
<b>Figure 4.27:</b> TGA instrumentation	122
<b>Figure 5.1 :</b> A graph showing the mass of wood and moisture content versus time	125
<b>Figure 5.2 :</b> Photograph of cold model experimental	126

<b>Figure 5.3</b> : Contour of volume fraction of CaO-sand mixture in CO <sub>2</sub> BFBAR (100 micron, 15 L/min)	127
<b>Figure 5.4</b> : Contour of volume fraction of CaO-sand mixture in CO <sub>2</sub> BFBAR (100 micron, 25 L/min)	128
<b>Figure 5.5</b> : Contour of volume fraction of CaO-sand mixture in CO <sub>2</sub> BFBAR (100 micron, 35 L/min)	128
<b>Figure 5.6</b> : Contour of volume fraction of CaO-sand mixture in CO <sub>2</sub> BFBAR (100 micron, 45 L/min)	129
<b>Figure 5.7</b> : Contour of volume fraction of CaO-sand mixture in CO <sub>2</sub> BFBAR (100 micron, 55 L/min)	129
<b>Figure 5.8</b> : Comparison between three particle sizes from FLUENT simulation	130
<b>Figure 5.9</b> : Graph comparison between FLUENT simulation and experimental (100 micron)	131
<b>Figure 5.10</b> : Graphs comparison between FLUENT simulation and experimental (500 micron)	132
<b>Figure 5.11</b> : Graphs comparison between FLUENT simulation and experimental (1000 micron)	132
<b>Figure 5.12</b> : The bell curve graph for bed expansion height	134
<b>Figure 5.13</b> : The effect of CaO-sand mixture ratio on bed expansion height (100 micron)	136
<b>Figure 5.14</b> : The effect of CaO-sand mixture ratio on bed expansion height (500 micron)	137
<b>Figure 5.15</b> : The effect of CaO-sand mixture ratio on bed expansion height (1000 micron)	138

<b>Figure 5.16:</b> The effect of CaO particle size on bed expansion height (40% CaO-sand mixture, 35 L/min)	139
<b>Figure 5.17:</b> The effect of air volume flow rate and pressure on bed expansion height (500 micron and 70% CaO mixture)	141
<b>Figure 5.18:</b> Rat holes formed during operation (15 L/min, 500 micron, 70% CaO mixture, 2 bars)	141
<b>Figure 5.19:</b> The effect of air volume flow rate and pressure on bed expansion height (1000 micron and 70% CaO mixture)	142
<b>Figure 5.20:</b> Amount of CaO entrained from CO <sub>2</sub> BFBAR (2 bar)	143
<b>Figure 5.21:</b> Amount of CaO entrained from CO <sub>2</sub> BFBAR (3 bar)	144
<b>Figure 5.22:</b> Amount of CaO entrained from CO <sub>2</sub> BFBAR (4 bar)	144
<b>Figure 5.23:</b> Amount of CaO entrained from CO <sub>2</sub> BFBAR (5 bar)	145
<b>Figure 5.24:</b> Amount of CaO entrained from CO <sub>2</sub> BFBAR (6 bar)	145
<b>Figure 5.25:</b> CaO mass exited rate (70% CaO and 55 L/min)	146
<b>Figure 5.26:</b> CaO mass exited rate (40% CaO and 55 L/min)	146
<b>Figure 5.27:</b> Pressure drop in CO <sub>2</sub> BFBAR using 2 bar pressurized air	149
<b>Figure 5.28:</b> Pressure drop in CO <sub>2</sub> BFBAR using 3 bar pressurized air	150
<b>Figure 5.29:</b> Pressure drop in CO <sub>2</sub> BFBAR using 4 bar pressurized air	151
<b>Figure 5.30:</b> Pressure drop in CO <sub>2</sub> BFBAR using 5 bar pressurized air	151
<b>Figure 5.31:</b> Pressure drop in CO <sub>2</sub> BFBAR using 6 bar pressurized air	151
<b>Figure 5.32:</b> CO <sub>2</sub> capture capacity for number 1 cycle of absorption /desorption process at 500, 600 and 700°C. Size: 1000 micron, $T_{desorption}$ 875°C for 20 min	153
<b>Figure 5.33:</b> CO <sub>2</sub> absorption rate for 1st and 2nd reaction stages in number 1 cycle of absorption/desorption process.	154

<b>Figure 5.34:</b> CO <sub>2</sub> capture capacity for number 4 cycle of absorption /desorption process at 500, 600 and 700°C. Size: 1000 micron, $T_{desorption}$ 875°C for 20 min	155
<b>Figure 5.35:</b> Cyclic desorption/absorption for 1000 micron CaO, desorption at 875°C with N <sub>2</sub> and absorbed at 600°C with 16% CO <sub>2</sub> , and balance N <sub>2</sub> .	156
<b>Figure 5.36:</b> CO <sub>2</sub> absorption rate of the desorption/absorption test	157
<b>Figure 5.37:</b> CO <sub>2</sub> absorption rate from the Equation 2.9 concluded by Abanades et al. (2003)	158
<b>Figure 5.38:</b> Amount of CO <sub>2</sub> detected by gas chromatograph (15 L/min, 650-750°C, 1000 micron)	159
<b>Figure 5.39:</b> Amount of CO <sub>2</sub> detected by gas chromatograph (45 L/min, 650-750°C, 1000 micron)	160
<b>Figure 5.40:</b> CO <sub>2</sub> detected by gas chromatograph (SPG)	163
<b>Figure 5.41:</b> Amount of CaO-sand mixture entrained	164
<b>Figure 5.42:</b> Gases detected by gas chromatograph (SPG)	165
<b>Figure 5.43:</b> Low heating value of SPG before and after CO <sub>2</sub> BFBAR	166
<b>Figure 5.44:</b> Low heating value of CPG before absorption process	168
<b>Figure 5.45:</b> CO <sub>2</sub> detected by gas chromatograph (CPG)	169
<b>Figure 5.46:</b> Amount of combustible gases detected by gas chromatograph (CPG)	170
<b>Figure 5.46:</b> LHV before and after CO <sub>2</sub> BFBAR	171



## LIST OF ABBREVIATIONS

atm	Atmosphere
BFB	Bubbling Fluidized Bed Gasifier
CFB	Circulating Fluidized Bed Gasifier
CFD	Computational Fluid Dynamics
CO <sub>2</sub> BFBAR	Bubbling fluidized bed CO <sub>2</sub> absorption reactor
CPG	Compressed Producer Gas
FLR	Fluidized limestone reactor
<i>g</i>	Gas
<i>HV</i>	Heating value
HyPr-PING	Hydrogen production by reaction-integrated novel gasification
IEA	International Energy Agency
LNG	Liquefied natural gas
MOX	Malaysia Oxygen Company
$P_{eq}$	Equilibrium decomposition pressure
<i>pg</i>	Producer gas
2D	Two Dimensional
3D	Three Dimensional
Q	Volume flow rate
RTP	Envergent Rapid Thermal Processing
S	Solid
SPG	Simulated Producer Gas
TCD	Thermal conductivity detector
$\Delta P$	Pressure drop

## LIST OF SYMBOLS

$A_r$	Aspect Ratio
$A$	Surface Area ( $m^2$ )
$B$	Constant in Syamlal-O'Brien drag model
$C_D$	Drag factor on single particle system
$Ca(OH)_2$	Calcium hydroxide
$CaCO_3$	Calcium carbonate
$CaO$	Calcium oxide
$CH_4$	Methane
$CO$	Carbon monoxide
$CO_2$	Carbon Dioxide
$d_i$	Inner diameter (m)
exp	Exponent
$e$	Restitution coefficient of solid phase
$F_{drag}$	The general drag force ( $kg/ms^2$ )
$g$	Gravity ( $m/s^2$ )
$g_o$	The general radial distribution function
$h$	Height (m)
$H_2$	Hydrogen
$h_s$	Static bed height (m)
$ln$	In
$\bar{I}$	The unit tensor
$K_{sg}$	Drag factor of phase s in phase g ( $kg/m^3s$ )

$L$	Length (m)
$W$	Width (m)
$H$	Height (m)
$N_2$	Nitrogen
$N$	Normal
$P$	Pressure (Pa)
$P_s$	Solids pressure (Pa)
$Re$	The Reynolds number
$Re_s$	The particle Reynolds number
$^{\circ}C$	Degree Celcius
$Out$	Out
$P$	Thermal Power (Watt)
$T$	Temperature ( $^{\circ}C$ )
$t$	Time (sec)
$u_{mf}$	Minimum fluidizing velocity (m/s)
$\rho$	Density ( $kg/m^3$ )
$\eta_{diesel}$	Efficiency of diesel engine
$d_s^{\bullet}$	Dimensionless particle size
$Ar_{numb}$	Archimedes number
$\mu_g$	Dynamic viscosity (kg/ms)
$m$	Mass (kg)
$A$	Cross sectional area ( $m^2$ )
$u_t^{\bullet}$	Dimensionless terminal velocity
$\Delta P$	Pressure drop (Pa)

$d_s$	Diameter solid particles size (m)
$\phi_s$	Sphericity of solid particle
$u_t$	Terminal Velocity (m/s)
$P_{inpg}$	Thermal power input (Watt)
%	Percent
(Na <sub>2</sub> CO <sub>3</sub> )	Sodium carbonate
(NaOH)	Sodium hydroxide
$\nabla \cdot q_s$	Diffusive flux of fluctuating energy (kg/ms <sup>3</sup> )
$\bar{V}$	Velocity (m/s)
$v_r$	The relative velocity correlation
$\varepsilon_g$	Gas phase volume fraction
$\varepsilon_s$	Solid phase volume fraction
$\gamma_{\Theta_s}$	Dissipation of granular temperature (kg/ms <sup>3</sup> )
$\Delta$	Change in variable, Final-Initial
$\nabla$	The Dell operator (1/m)
$\Theta_s$	Granular temperature (°C)
$\lambda_s$	Bulk viscosity (kg/ms)
$\mu_g$	Gas viscosity (kg/ms)
$\mu_s$	Granular viscosity (kg/ms)
$\mu_{s,col}$	Collisional viscosity (kg/ms)
$\mu_{s,kin}$	Kinetic viscosity (kg/ms)
$\mu_{s,fric}$	Frictional viscosity (kg/ms)
$\Pi$	The irrational number $\Pi$

$P_g$	Gas density ( $\text{kg/m}^3$ )
$P_s$	Solid density ( $\text{kg/m}^3$ )
$\overset{=}{\tau}$	The stress-strain tensor (Pa)

# **PENINGKATAN KUALITI GAS TERHASIL MELALUI SERAPAN CO<sub>2</sub> MENGUNAKAN CAMPURAN CaO – PASIR DI DALAM REAKTOR LAPISAN TERBENDALIR**

## **ABSTRAK**

Tesis ini adalah mengenai kajian ujikaji bagi meningkatkan kualiti gas yang dihasilkan dari proses penggasan melalui konsep penyerapan karbon dioksida (CO<sub>2</sub>) menggunakan campuran kalsium oksida (CaO) bersama pasir di dalam reaktor penyerapan lapisan terbendalir gelembung CO<sub>2</sub> (CO<sub>2</sub> BFBAR). Selain itu kajian ini juga menggunakan kaedah simulasi berangka. Pada masa kini, penggasan biojisim merupakan satu alternatif yang dapat digunakan untuk menggantikan tenaga bahanapi fosil. Gas terhasil, yang terhasil daripada proses penggasan biojisim boleh digunakan untuk menjanakan kuasa dan elektrik. Walaubagaimanapun, CO<sub>2</sub> yang terdapat di dalam gas terhasil mengurangkan nilai pemanasannya kerana CO<sub>2</sub> bertindak sebagai bahan pencair. Penggunaan batu kapur yang mengandungi terutamanya bahan mineral kalsit (kalsium oksida) sebagai bahan pengerap berasaskan kalsium untuk menyerap CO<sub>2</sub> yang terdapat di dalam gas terhasil boleh menjadikan teknologi biojisim ini lebih berdaya maju. Pengisian dinamik bendalir berkomputer (CFD) 3 dimensa digunakan untuk melakukan simulasi bagi mencari ciri-ciri hidrodinamik bagi bahan lapisan CaO-pasir yang diletakkan dalam CO<sub>2</sub> BFBAR. Keputusan simulasi yang diperolehi bagi CaO bersaiz 100, 500 dan 1000 micron menunjukkan bahawa pembendaliran terhasil dengan baiknya pada kadar alir isipadu 15-55 L/min menggunakan udara. Selain itu, CO<sub>2</sub> BFBAR juga telah dibangunkan dan kajian terhadapnya pada kelakuan bahan campuran CaO-pasir juga dilihat dari sudut ujikaji model sejuk. Kesan-kesan disebabkan oleh

campuran CaO-pasir, saiz zarah CaO, kadar aliran isipadu dan tekanan masukan udara disiasat secara ujikaji. Proses penyerapan-nyahserapan oleh CaO juga dikaji menggunakan Penganalisa Termogravimetri (TGA) terhadap 1 kitar, 4 kitar dan kitar berbagai. Tiga suhu yang berbeza (500, 600 dan 700°C) disetkan sebagai pembolehubah. Kadar tindakbalas CaO diperolehi. Keputusan menunjukkan pada kitar pertama, kadar tindakbalas penyerapan CO<sub>2</sub> adalah cepat semasa di peringkat pertama kemudian diikuti dengan kadar tindakbalas penyerapan yang perlahan. Sebanyak 0.337 dan 0.065 mg/min kadar tindakbalas penyerapan CO<sub>2</sub> didapati untuk kawasan penyerapan pantas dan perlahan. Diperhatikan juga bahawa kadar tindakbalas penyerapan CO<sub>2</sub> berkurangan apabila bilangan kitar penyerapan-nyahserapan ditambah. Selepas ujikaji TGA dijalankan, ujikaji model panas pula dilakukan untuk mengkaji kebolehesanan penyerapan CO<sub>2</sub> menggunakan nilai-nilai optimum yang diperolehi dari ujikaji model sejuk. Gas simulasi yang terdiri daripada 20% CO<sub>2</sub> dan 80% N<sub>2</sub> digunakan dalam CO<sub>2</sub> BFBAR sepanjang suhu 650-750°C. Pembendaliran terhasil dengan baiknya pada keadaan 50 dan 40 peratus campuran CaO bagi semua tekanan (2-6 bar). Saiz zarah 1000 micron pada campuran CaO-pasir dan kadar aliran isipadu udara antara 15-55 L/min juga memberikan pembendaliran yang baik. Di dalam ujikaji model panas pula, penyerapan CO<sub>2</sub> yang baik terhasil pada keadaan campuran 50% CaO menggunakan tekanan gas simulasi pada nilai 3 bar dengan kadar alir isipadu 45 L/min sepanjang suhu 650-750°C dalam CO<sub>2</sub> BFBAR. Penggunaan gas terhasil simulasi dan gas terhasil bertekanan juga menunjukkan keputusan yang baik. Kepekatan CO<sub>2</sub> dalam gas terhasil simulasi menurun kepada 57.5%, manakala hidrogen dan karbon monoksida pula meningkat kepada 12% dan

6% selepas beroperasi selama 10 minit. Apabila menggunakan gas terhasil bertekanan, kepekatan CO<sub>2</sub> juga menurun sebanyak 77.4%, manakala hidrogen dan karbon monoksida pula meningkat kepada 23.3% dan 21.7%. Oleh sebab itu, nilai pemanasan gas terhasil bertekanan secara langsung juga meningkat dari 4.51 MJ/Nm<sup>3</sup> kepada nilai semaksimum 6.04 MJ/Nm<sup>3</sup> iaitu peningkatan sebanyak 38%.



**ENHANCEMENT OF PRODUCER GAS QUALITY THROUGH CO<sub>2</sub>  
ABSORPTION USING CaO-SAND MIXTURE IN A FLUIDIZED BED  
REACTOR**

**ABSTRACT**

This thesis concerns an experimental study and numerical simulation used to enhance the producer gas quality through carbon dioxide (CO<sub>2</sub>) absorption using calcium oxide (CaO) - sand mixture in a CO<sub>2</sub> bubbling fluidized bed absorption reactor (CO<sub>2</sub> BFBAR). Biomass gasification is a thermo-chemical conversion process of solid biomass into gaseous fuel called producer gas that can be used to generate power and electricity. However, carbon dioxide (CO<sub>2</sub>) content in the producer gas reduces its heating values as CO<sub>2</sub> acts as a diluent. The use of limestone consisting mainly of the mineral calcite (calcium oxide, CaO) as calcium based sorbent to absorb CO<sub>2</sub> in the producer gas will increase the heating value of the producer gas. 3-D Computational Fluid Dynamics (CFD) software was used to determine hydrodynamic characteristic of CaO-sand bed material in a CO<sub>2</sub> BFBAR. The simulation results show that with 100, 500 and 1000 micron particle size of CaO, good fluidization at 15 – 55 L/min volume flow rate of air was achieved. The CO<sub>2</sub> BFBAR was developed and the behavior of CaO-sand mixtures in a cold model experiment was studied. The effect of the CaO-sand mixtures, the CaO particle sizes, the volume flow rate and the pressure of air intake were investigated experimentally. The absorption-desorption process of CaO was studied with the thermogravimetric analyzer (TGA) over 1, 4 and a muticycle. Three different temperatures (500, 600 and 700°C) were set as variables. The reaction rate of CaO was obtained. Results show that for number 1 cycle the CO<sub>2</sub> absorption

reaction rate was fast at first stage and then followed with slower reaction rate. About 0.337 and 0.065 mg/min CO<sub>2</sub> reaction rate were obtained in rapid and slow absorption regime respectively. It is also observed that the CO<sub>2</sub> absorption reaction rates decreases when number of cycle's desorption-absorption process was increased. After TGA experiment, the hot model experiment was conducted to investigate CO<sub>2</sub> absorption at the optimum condition obtained from the cold model experiment. The simulated gas consisting of 20% CO<sub>2</sub> and 80% N<sub>2</sub> was introduced in the CO<sub>2</sub> BFBAR at temperatures of 650-750°C. The CaO percentages of 50 and 40 in sand were found to have a good fluidization at all air pressures (2 - 6 bar). In addition to that, the 1000 micron particle size of the CaO-sand mixture and the volume flow rate of air between 15 – 55 L/min were also found to generate good fluidization. In the hot model experiment, the best CO<sub>2</sub> absorption occurs in 50% CaO mixture with simulated gas, at pressure of 3 bar and the volume flow rate of 45 L/min at 650-750°C in the CO<sub>2</sub> BFBAR. The CO<sub>2</sub> concentration in the simulated producer gas when applied decreases approximately 57.5%, where this resulted in increases of H<sub>2</sub> and CO to approximately 12% and 6%, respectively within 10 minutes of operation. For the compressed producer gas, the CO<sub>2</sub> concentration decreases approximately 77.4%, where H<sub>2</sub> and CO increase approximately 23.3% and 21.7%, respectively. Therefore the heating value of the compressed producer gas increases from 4.51 to maximum of 6.04 MJ/Nm<sup>3</sup> an increase of 38%.

## **CHAPTER ONE**

### **INTRODUCTION**

#### **1.1 Fuel Scenario in Malaysia**

Fuel is undoubtedly the most important source of energy. It has been used predominantly in power plants and to generate work in internal combustion engines. However, the extensive exploitation of fossil fuels for power has given rise to a number of serious problems namely depletion of fuel reserves, price inflation of raw materials, adverse effects on the environment due to emissions from combustion devices and increment of greenhouse gas emissions.

Malaysia is currently known as a significant producer of oil and its oil reserves is the third highest in the Asia-Pacific region after China and India. Interestingly, Malaysia is a net exporter of liquefied natural gas (LNG) and is known as the third largest in the world after Qatar and Indonesia in 2010 (Energy Information Administration Report, 2011). According to Oil and Gas Journal (2011), in January 2011, Malaysia had proven to have oil reserves of 4.0 billion barrels. Although the oil reserves are large, it is decreasing from a peak of 4.3 billion barrels in 1996 as shown in Figure 1.1. In terms of oil production in Malaysia, it is reducing but from there is an increase in consumption (Figure 1.1, below). These unparalleled situations will cause the country's oil reserves to become exhausted in the future unless new explorations show positive results.

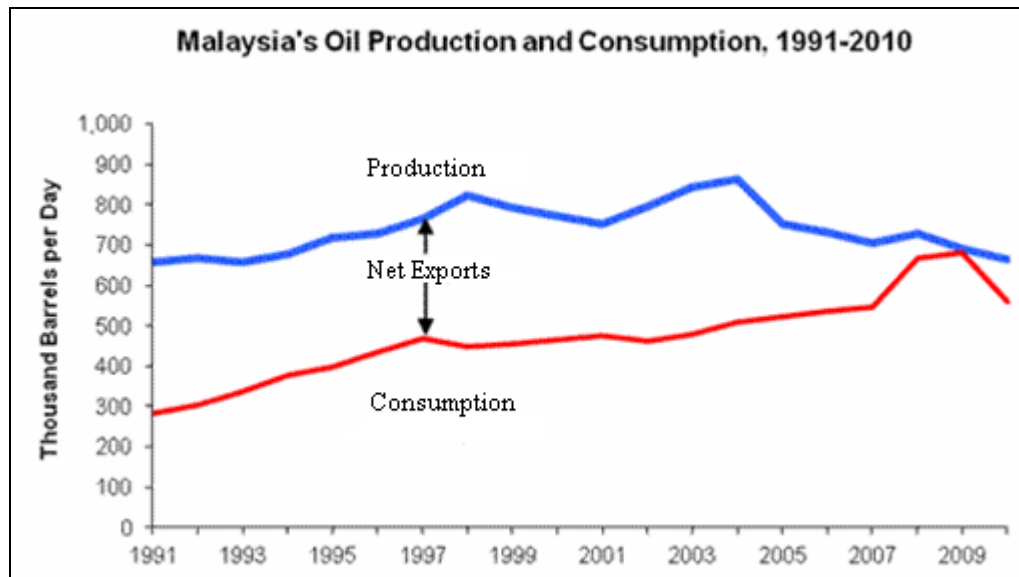
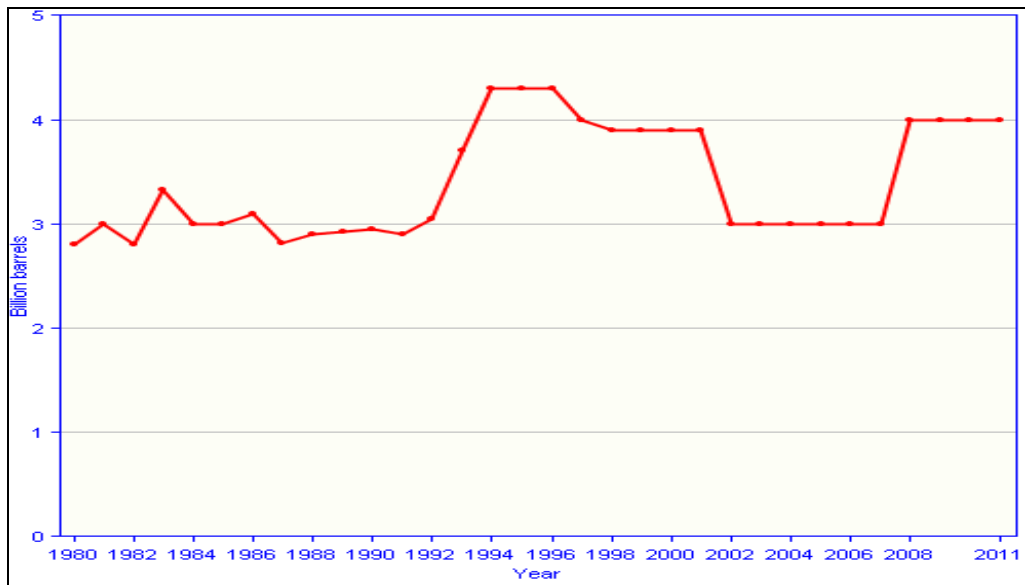


**Figure 1.1-** Malaysia oil reserves (Top), Malaysia oil production and consumption (below) (EIA, 2011)

Growing demand for crude oil or petroleum (element in fossil fuel) in Malaysia which is set to become a developed nation by 2020 will result in higher energy cost and greater dependence on imported oil given the current crude oil capacity (Bari *et al.* 2011). This can have a potential negative impact on the nation's economic growth as rising commodity prices are closely tied to

inflation rates. That is why many developed as well as developing countries, Malaysia included, have tried to utilize alternative and renewable sources of energy.

Renewable energy offers opportunity to lower fossil fuel consumption. Energy derived from solar, wind, wave, tidal, hydroelectric, geothermal and biomass sources are considered renewable. Because most forms of renewable energy are derived either directly or indirectly from the sun, there is abundant supply of renewable energy available, unlike fossil fuels. The use of renewable energy also provides environmental, economic and political benefits, and they are also not subjected to depletion in time. One of the fuels for renewable energy is biomass.

## **1.2 Biomass**

Biomass is the most abundant resources and available in all parts of Malaysia. It has the potential to be one of the best options for providing on demand renewable fuel that can be utilized in various energy conversion technologies and also has the advantage of being carbon sink without contributing to the net production of carbon dioxide, CO<sub>2</sub>. Biomass is defined as organic materials existing in all plants and animals such as forest and mill residues, wood wastes, agricultural crops and wastes, animal wastes and municipal solid wastes.

Malaysia abundant biomass wastes come from its wood, oil palm and agro-industries. Malaysia produces more than 70 million tones per year of biomass wastes worth RM 23 million annually. Over the next 20 years, palm oil industry is expected to expand by 40%, hence the value of residues from wood and oil palm is estimated to be about RM 500 million by 2020. Of these residues, wood waste, shells, empty fruit bunch and fibres provide the greatest potential for commercial operations (Malaysia Energy Centre, 2008). For instance, in year 2011 Malaysia used Envergent Rapid Thermal Processing (RTP) technology to perform the engineering design to convert palm biomass to renewable heat and electricity. This RTP facility will complete in early 2013, and it will be Malaysia first plant to use RTP for the production of a clean-burning liquid biofuel derived from biomass for the purpose to generate renewable electricity and heat (PR Newswire, 2011).

In biomass technologies, there are two main processes for converting biomass sources into useful forms of energy: thermochemical and biochemical/biological chemistry (McKendry, 2002b). In thermochemical conversion, there are four processes: combustion, pyrolysis, gasification and liquefaction. In this research study only the thermochemical in particular gasification process will be focused. Figure 1.2 shows the thermochemical process, intermediate energy carriers and final energy products resulting from the thermochemical conversion.

Biomass gasification is a technology to produce low to medium energy fuel gas (Klass, 1998) for internal combustion engines or coupled to turbines to generate power. Gasification is defined as the thermochemical conversion of carbonaceous feedstocks such as biomass and coal into producer gas or synthesis gas (syngas - composed primarily of hydrogen and carbon monoxide) using air, oxygen or steam to react with the solid fuel at high temperature, typically in the range of 800-900°C. Only inert ashes by products are produced at the end of the process. According to Rezaiyan (2005) and McKendry (2002b), the producer gas produced has heating value (*HV*) around 4-6 MJ/Nm<sup>3</sup>.

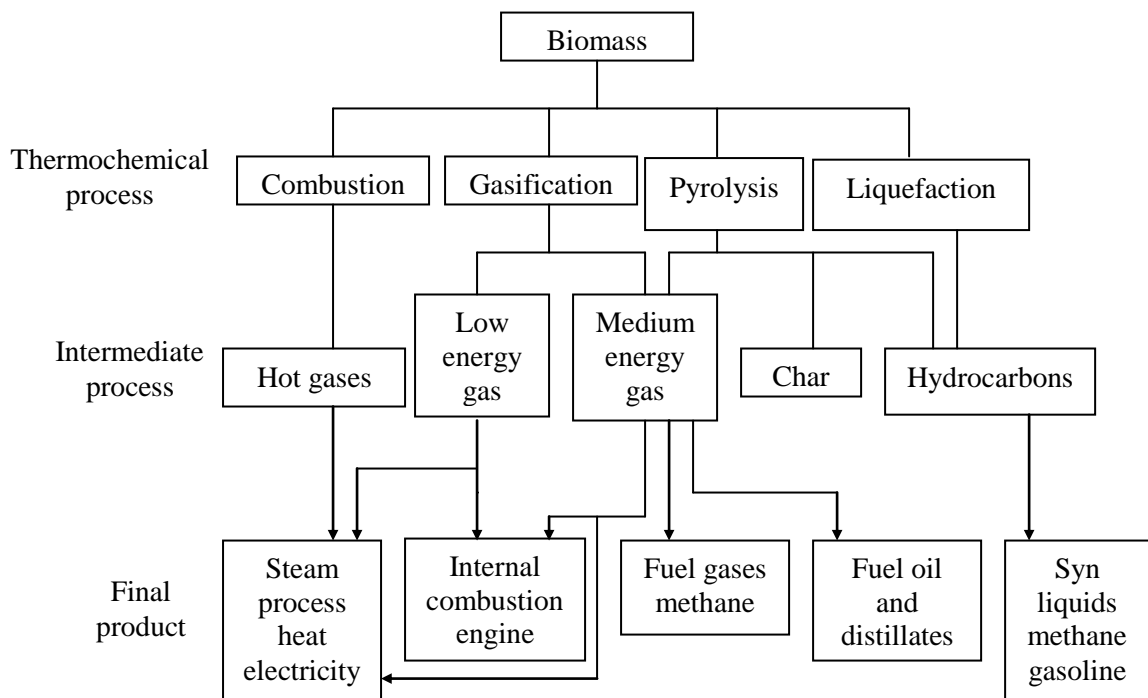


**Figure 1.2:** The thermochemical processes and products.

(McKendry, 2002b)

### 1.3 Carbon Dioxide Capture

Carbon dioxide (CO<sub>2</sub>), which is containing in producer gas-air mixture is only 9-15% carbon dioxide, and others are hydrogen (15-20%), carbon monoxide (10-15%), methane (3-5%) and 40-50% of nitrogen by volume (Sen, 2005 and Reed, 1988). CO<sub>2</sub> content in the producer gas reduces its heating values as CO<sub>2</sub> acts as a diluent. Removing CO<sub>2</sub> from the producer gas will inadvertently increase its heating value. It will also improve the percentage of its hydrogen and all combustible gas contents.

Recently, there are a few methods have been proposed for CO<sub>2</sub> capture. The methods for capturing CO<sub>2</sub> from flue gases are membrane separation (Dindore *et al.*, 2004), cryogenic fractionation (Khoo *et al.*, 2006), and solvent absorption (Al-Juaied *et al.*, 2006), either physical or chemical sorption on solid surfaces (Gupta *et al.*, 2002). However, these two methods such as membrane separation and cryogenic fractionation have not favored for CO<sub>2</sub> separation. Example membrane separation systems, even though are highly efficient and have been employed for the separation of CO<sub>2</sub>, but due to their complexity, high energy cost, and limited performance, membrane systems are not entirely well suited. As well as cryogenic fractionation systems, it also required high energy requirements.

Solvent absorption, on the other hand is well recognized. It is using various solvents, for instance, Selexol (Kohl *et al.* 1997) as a physical solvent or mono-ethanol amine (MEA) (Filburn *et al.*, 2005) as a chemical solvent. However, according to Rao *et al.* (2002) severe energy penalties and the high



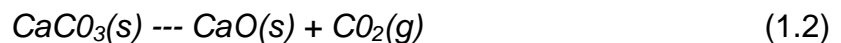
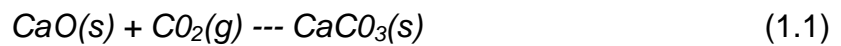
cost of the system are significant disadvantages of the method especially on the use of amine. The low concentration of CO<sub>2</sub> in the flue gases at atmospheric pressure and low temperature (40 - 150°C) required for the absorption and solvent recovery process leading to the high cost of system.

The only one of the most promising method is based on the reversible absorption of CO<sub>2</sub> on specific metal oxides at high temperature. CO<sub>2</sub> capture using sorbents based on the oxides of calcium (Manovic *et al.*, 2009), potassium (Lee *et al.*, 2006), lithium (Fauth *et al.*, 2005), sodium (Knuutila *et al.*, 2009) and magnesium (Lee *et al.*, 2008) have been reported. The most have attention owing among these is calcium oxide (CaO) based sorbents because of their wide availability, low cost, higher absorption capacity and high selectivity for CO<sub>2</sub>.

According to Chen *et al.* (2009), Alvarez *et al.* (2007), Lu *et al.* (2008) and Akiti *et al.* (2002), precursors such limestone (also known as Calcium Carbonate, CaCO<sub>3</sub>), dolomite, calcium acetate and calcium sulphate hemihydrate can be processed to derive CaO. Among these, the most common CaO precursors are limestone. This is because of the availability and low cost of limestone as mention. According to Zulasmin (2007), Malaysia country is blessed with abundant reserve of limestone resources. Extensive limestone resources are located in the states of Perak, Pahang, Kelantan, Kedah and Negeri Sembilan. It was estimated over 10 billion tonnes of limestone resources throughout the country. Example in the state of Perak, there is a 0.0405 km<sup>2</sup> limestone quarry and it estimated limestone reserve of 4

million tones. With current monthly usage of 5000 tonnes per month, the quarry can provide raw limestone for the next 66 years (Zantat 2009). Talking about the price of raw limestone, it is sold for only RM60 a tonne compared to processed and value-added limestone that can fetch around RM390 a tonne, according to Elan (2011).

The reaction of solid CaO with CO<sub>2</sub> can be shown as in Equation 1.1 called absorption, and this is a spontaneous exothermic process at ambient conditions. At elevated temperatures, the reversed endothermic reaction called desorption (Equation 1.2) occurs.



In theory the reactions in Equations 1.1 and 1.2 are fully reversible; thus, they can be appropriated to capture CO<sub>2</sub> from producer gas and upon desorption, CO<sub>2</sub> will be released. The cycle of desorption and absorption is repeated over and over. For such a process, two situations and temperatures are employed. Desorption is performed at higher temperature above 800°C and absorption at temperature below 800°C. The absorption–desorption reaction will be discussed in detail in Section literature.

#### 1.4 Problem Statements

The need for doing research on biomass sources is due to the fossil fuels is non-renewable. They are limited in supply and will one day be depleted. By 2050, the depletion of fossil fuels is expected to be worse and alternative fuels have to be discovered (Takuyuki Yoshioka *et al.*, 2005). Hence the search for alternative energy sources for sustaining energy requirement by human beings must be done because the depletion of fossil fuels is occurring at a faster rate due to increasing gap between demand and production of fossil fuels. This problem is the foremost reason why renewable sources of energy must be studied.

The fossil fuels combustion emits carbon dioxide (CO<sub>2</sub>), a green house gas will contributes to global warning. Magnus *et al.* (2006) wrote that CO<sub>2</sub> concentration in the atmosphere is 30% higher than it was before the industrialization era and the annual emissions are still increasing today. To overcome this problem, renewable energy sources such as biomass can be used as fuel. Burning biomass contributes no net CO<sub>2</sub> to the atmosphere because replanting biomass will absorbs the CO<sub>2</sub>.

The unused biomass wastes are abundant whilst managing them is difficult and expensive without any added value. According to Wan Asma *et al.* (2010), unused biomass wastes are collected more than 15 million tonnes per year. The wastes can be used as fuel to generate energy with added value.

Producer gas has small hydrogen concentration, approximately 6-20% by volume when using a downdraft biomass gasifier (Munoz *et al.*, 2000; Sridhar *et al.*, 2001; Zainal *et al.*, 2002; Dogru *et al.*, 2002; Adnan *et al.*, 2002 and Uma *et al.*, 2004). To increase the percentage of the hydrogen, a new method has to be studied and developed. For instance, the producer gas from biomass gasification system contains high amount of CO<sub>2</sub>, 15-20% (Sridhar *et al.* 2001 and Dogru *et al.* 2002) thereby lower its heating value as CO<sub>2</sub> acts as a diluent. Removing CO<sub>2</sub> from the producer gas will improve its heating value. The heating value of producer gas will be expected to increase from 4 MJ/Nm<sup>3</sup> to about 6 MJ/Nm<sup>3</sup>. This will not just improve its heating value but inadvertently improve the amount of combustible gases such as hydrogen, carbon monoxide and methane.

With these problems statement, there are two contributions can be raised up. The first is the improvement of compressed producer gas-air from downdraft gasifier. As mentioned in literature section, there appears no systematic study on the useage of CaO-sand mixture for CO<sub>2</sub> absorption process by CaO in downdraft gasifier application. The second contribution is the study of CO<sub>2</sub> absorption in the CO<sub>2</sub> BFBAR. The concept of the kinetic reaction between CaO and CO<sub>2</sub> are focused. Therefore, there is still room for researchers to study the concept, development and application of CO<sub>2</sub> absorption by CaO to producer gas from the downdraft gasification process for future use, particularly in improving the quality of producer gas.

## 1.5 Research Objectives

The main objective of the work presented in this thesis is to enhance the quality of the producer gas using CaO as absorbent reagent mixed with sand. The CO<sub>2</sub> gas contained in the producer gas is absorbed via a reactor known as bubbling fluidized bed CO<sub>2</sub> absorption. The sub-objectives are:

- To simulate the hydrodynamic characteristic of a bubbling fluidized bed CO<sub>2</sub> absorption reactor using computer software, FLUENT.
- To design and develop a bubbling fluidized bed CO<sub>2</sub> absorption reactor.
- To conduct cold study to characterize the hydrodynamic behavior of the system using CaO – sand mixtures.
- To characterize the bubbling fluidized bed CO<sub>2</sub> absorption reactor using absorption – desorption process with the electric ceramic heater band.
- To determine the CO<sub>2</sub> absorption reaction rate of CaO using Thermogravimetric analysis (TGA).
- To test and analyze the bubbling fluidized bed CO<sub>2</sub> absorption reactor with simulated producer gas (SPG) and actual compressed producer gas (CPG) from downdraft gasifier.

## **1.5 Research Scope**

The scope of the research can be divided into four stages as follows:

1. Study on calcium oxide as absorbent of CO<sub>2</sub> gas, focusing on absorption – desorption processes.
2. Study on the 3-D computational fluid dynamics software such as FLUENT to simulate the hydrodynamic phenomena of CaO in the bubbling fluidized bed CO<sub>2</sub> absorption reactor (CO<sub>2</sub> BFBAR).
3. Study on the development of the bubbling fluidized bed CO<sub>2</sub> absorption reactor based on the principles of bubbling fluidization.
4. Study on the biomass material such as furniture wood and the process of gasification, focusing on the small downdraft gasifier.

## **1.7 Organization Chapters**

Chapter 1 contains the overview and the direction of the study. It highlights the background of the research in which the scenario of fuel in Malaysia is discussed, followed by an introduction on biomass and CO<sub>2</sub> gas capture. Problems statement explaining the reasons why this research is done and the contributions are also clearly stated. The objectives and scopes of the research are listed to provide preliminary knowledge about the direction of this project.

Chapter 2 contains relevant theories, concepts and literature review of past researches to strengthen the framework of the research. Various elements associated with biomass are described. The detail of absorption process of carbon dioxide and the simulation method obtained from other researchers are also listed and discussed.

Chapter 3 represents the design and development of a bubbling fluidized bed CO<sub>2</sub> absorption reactor (CO<sub>2</sub> BFBAR). The dimensions of the CO<sub>2</sub> BFBAR are shown and thoroughly described.

The experimental setup, procedures and experimental studies are detailed in Chapter 4. The description of the apparatus and their usage are also included.

The results and discussion of the experiments conducted are presented in Chapter 5. All results obtained are arranged in tables, graphs and figures, and carefully laid out for easy reference. Operations of the moisture content test, bomb calorimeter test, 3-D FLUENT simulation, statistical analysis, gasifier experiment, cold model, thermogravimetric analysis (TGA) and hot model experiment for the CO<sub>2</sub> absorption are also stated and discussed.

Finally in Chapter 6, summarizes and concludes the findings of the study are made and recommendations suggested for future work are listed to complete the thesis.

## **CHAPTER TWO**

### **LITERATURE REVIEW**

#### **2.1 Introduction**

In this chapter, a literature review has been done on the types of gasifier and chemical conversion of biomass material via the gasification process into gaseous fuel. This includes an elaboration on the combustible components of the gas, as well as the work of other researchers on the process of increasing the percentage of hydrogen, the absorption process of CO<sub>2</sub> and simulation method.

#### **2.2 Biomass Gasification**

Biomass is a non-fossil, energy-containing form of carbon and includes all land and water based vegetation. It is the only indigenous renewable energy resource that is capable of displacing large amounts of solid, liquid and gaseous fossil fuels. Biomass can be used for generating electric power and industrial processes. One of the methods used to convert biomass into useful form of energy is called gasification, producing combustible gas, which can be used in internal combustion engines. The gases typically consist of hydrogen (H<sub>2</sub>), carbon monoxide (CO), methane (CH<sub>4</sub>), carbon dioxide (CO<sub>2</sub>) and nitrogen (N<sub>2</sub>) commonly named as “producer gas”. According to Zhang *et al.* (2004), biomass when burnt or gasified will produce dirty raw gas mixture or producer gas composed of hydrogen, carbon monoxide, carbon dioxide, water, methane and various light hydrocarbons along with undesirable dust



(ash and char), tar, ammonia, alkali (mostly potassium) and some other trace contaminants.

### **2.2.1 Types of Gasifier**

The gasification process occurs in a reactor called gasifier. There are basically two types of gasifiers: fixed bed and fluidized bed. The fixed bed gasifier has been the traditional process used for gasification and operates at high temperature around 1000°C. It can be classified as downdraft, updraft and cross flow, depending on the direction of the flow (McKendry, 2002c).

### **2.2.2 Fixed Bed Gasifier**

A downdraft gasifier, where the biomass feed and air move in the same direction or co-current. The product gases leave the gasifier after passing through the hot zone, enabling partial cracking of the tar formed during gasification and leaving a producer gas with low tar content. The overall energy efficiency of the downdraft gasifier is low because the gases leave the gasifier unit at a high temperature of 900-1000°C and due to the high heat content carried over by the hot gas (McKendry, 2002c). Figure 2.1 shows a diagram of a downdraft gasifier.

In an updraft gasifier, biomass feed is introduced at the top and the air flows from the bottom of the unit via a grate in a counter current flow. The solid char forms higher up the gasifier above the combustion zone. An updraft gasifier is simple in design and can handle biomass with high moisture

content up to 50% by weight (McKendry, 2002c). Figure 2.2 shows a diagram of an updraft gasifier.

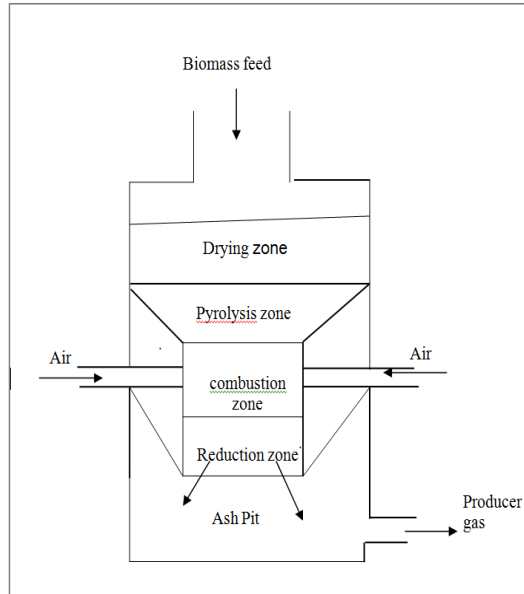


**Figure 2.1:** Diagram of a downdraft gasifier

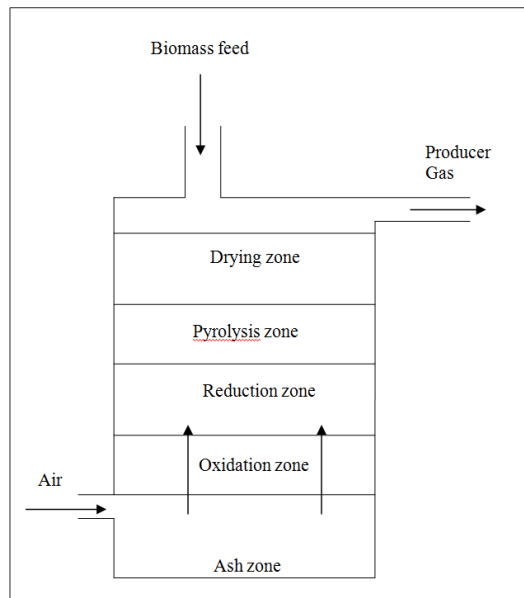


**Figure 2.2:** Diagram of an updraft gasifier

The gasifier where the air is introduced from the side while the feed biomass moves downwards is called cross flow gasifier. The producer gas is drawn from the opposite side of the unit at the same level of the air introduced. A hot gasification zone forms around the entrance of the air, with the pyrolysis and drying zones being formed higher up in the vessel. Ash is removed at the bottom and the temperature of the gas leaving the unit is 800-900°C. This gives low overall energy efficiency for the process and a gas with high tar content (McKendry, 2002c). Figure 2.3 shows the diagram of a cross flow gasifier.

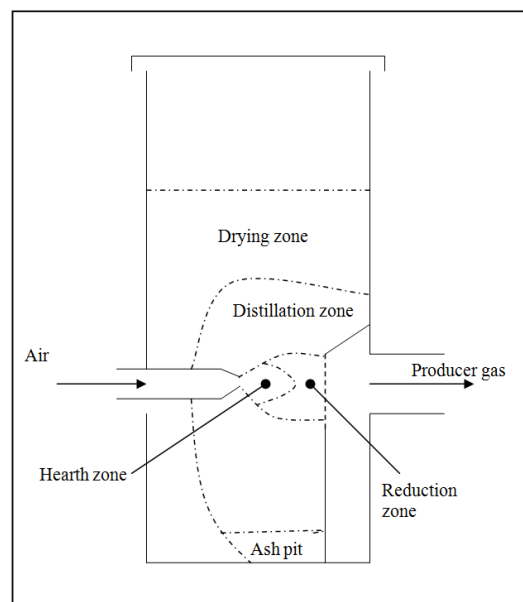


**Figure 2.3:** Diagram of a cross flow gasifier

### 2.2.3 Fluidized Bed Gasifier

The fluidized bed gasifier has been used extensively for coal gasification for many years (Garcia-Ibanez *et al.*, 2001). It is favored by many gasifier designers for using smaller feedstock sizes. In the gasification zone of the fluidized bed, a uniform temperature distribution is achieved. There are

two main types of fluidized bed gasifier that can be classified as: bubbling fluidized bed and circulating fluidized bed (Fouilland *et al.*, 2010 and McKendry, 2002c).

A bubbling fluidized bed gasifier (BFB) consists of a vessel with a grate at the bottom through which air is introduced. Above the grate is the fluidized bed of fine-grained materials into which the prepared biomass feed is introduced. The BFB utilizes minimum fluidization velocity of sand and fine-grained bed material to achieve fluidization state. The sand acts as a heat transfer medium. The ash entrained out of the gasifier is collected in a cyclone separator. For biomass material with high moisture content and low heating value, BFB is recommended (Ciferno and Marano, 2002). A detailed concept of the BFB will be discussed in Section 3.2 and the diagram of the bubbling fluidized bed is shown in Figure 2.4 (a).

A circulating fluidized bed is suitable for waste fuels with a high percentage of non-combustibles (heating value 5 - 35 MJ/kg). It operates at a temperature around 800-900<sup>0</sup>C (McKendry, 2002c). Crushed coal along with sorbent (limestone) is fed to the lower furnace where it is kept suspended and burnt in an upward flow of combustion air. The sorbent is fed to facilitate capture of sulphur from the coal in the bed itself resulting in consequent low sulphur emission. Due to high gas velocities, the fuel ash and unburnt fuel are carried out of the combustor with the flue gases. These are then collected by a recycling cyclone separator and returned to the lower part of the gasifier. Figure 2.4 (b) shows a diagram of a circulating fluidized bed.

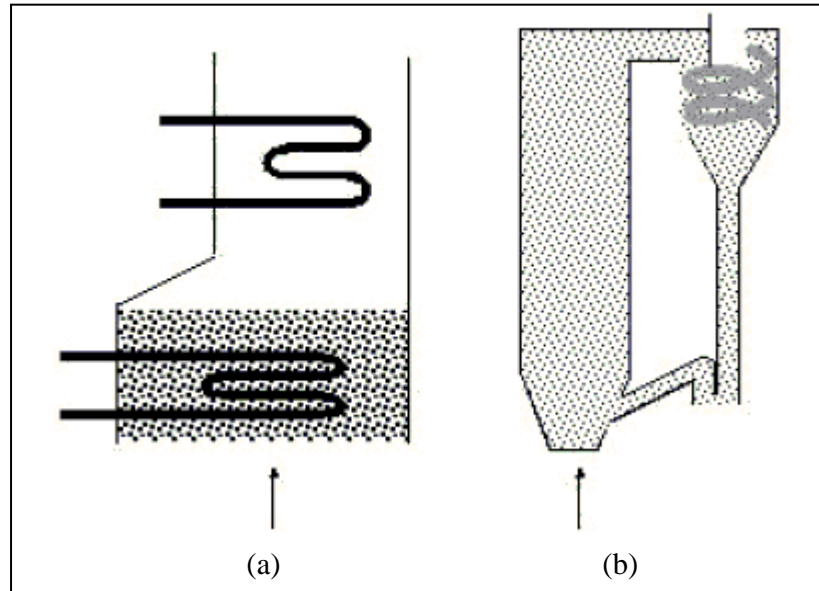
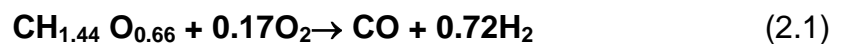


**Figure 2.4:** Diagram of a) bubbling bed. b) circulating bed

#### 2.2.4 Wood Gasification

Wood is an example of biomass source. It is composed of cellulose, hemicellulose, and lignins (Lee 1996). It is defined as lignocellulosic material. The structures of hemicellulose and lignins are very complicated, which contribute to the complexity of the thermochemical conversion reactions. Consider wood with a chemistry formula  $\text{CH}_{1.44} \text{O}_{0.66}$ , and the ideal gasification reaction with oxygen can be written as follows:



This ideal gasification reaction is an endothermic process, which means the reaction in the system absorbs energy from the surroundings in the form of heat. Oxygen is partially supplied to gasify the wood and produce carbon monoxide and hydrogen. According to Reed (1988), the surplus oxygen reacts with about a third of the CO and H<sub>2</sub> ideally produced. The Equation 2.2 is the theoretical global gasification reaction with CO<sub>2</sub> and H<sub>2</sub>O as additional products.



Biomass materials, wood will undergo three stages of mass loss in the gasification process. The stages are drying, pyrolysis and gasification. Inherent moisture in the biomass is removed in the drying stage. The temperature rises and the biomass particles begin to decompose and release volatiles. When this happens it is called the pyrolysis stage. In the last stage, where there is insufficient oxygen supplied, partial oxidation takes place. Under this condition, partial oxidation of the residues and volatiles occurs. This results in the generation of partially oxidized products and combustible gases such as hydrogen, carbon monoxide and methane. These stages occur rapidly.

The amount of water depends on wood species and most species can absorb about 30% water (U.S. Departments of Agriculture, 2007). According to McKendry (2001), moisture content of wood more than 30% makes ignition

difficult and will reduce heating value of the producer gas due to the need to evaporate additional moisture before combustion occurs. So to improve heating value of the producer gas, moisture content of the wood must be kept below 30%.

### **2.2.5 Producer Gas Composition from a Downdraft Gasifier**

The producer gas consists of combustible and incombustible gases. Theoretically, the composition of producer gas-air mixture is 15-20% hydrogen, 10-15% carbon monoxide, 9-15% carbon dioxide, 3-5% methane and 40-50% nitrogen by volume (Sen, 2005 and Reed, 1988).

Gunderson and Darren (2000) reported that hydrogen could be obtained from biomass and many other compounds such as water and fossil fuels. To obtain hydrogen from biomass, pyrolysis or gasification must be applied, which typically produces a gas containing 20% hydrogen by volume, which can be further steam-reformed to make higher quality gas.

Munoz *et al.* (2000) stated that producer gas contained 14% hydrogen, 22% carbon monoxide, 13% carbon dioxide, 3% methane and rest, nitrogen that had been determined from wood residues using a downdraft fixed bed gasifier. In their research, they used two fuels, producer gas and gasoline to measure the performance of a spark ignition engine. The results showed that there was so much loss of power in using producer gas compared with gasoline. The hydrocarbon and carbon monoxide were also reduced but carbon dioxide increased when using producer gas.

Sridhar *et al.* (2001) also stated that the producer gas can be fuelled into a spark ignition engine converted from a diesel engine. They used open top downdraft gasifier system to convert biomass (causurina species wood) into producer gas. The composition of the producer gas was 19% hydrogen, 19% carbon monoxide, 12% carbon dioxide, 2% methane, 2% water and rest, nitrogen. They found that the performance of the engine at higher compression engine had been smooth and the cylinder pressure-crank angle trace had shown smooth pressure variations during the entire combustion process without any sign of abnormal pressure raise.

Zainal *et al.* (2002) reported that the gas composition found in their experiment on a downdraft biomass gasifier using furniture wood and wood chips was 14.05% hydrogen, 24.04% carbon monoxide, 14.66% carbon dioxide, 2.02% methane, 1.69% oxygen and 43.62% nitrogen.

Dogru *et al.* (2002) also investigated gasification potential of hazelnut shells using a downdraft gasifier. They obtained a gas composition of 11.11%-14.77% hydrogen, 8.56%-18.56% carbon monoxide, 9.52%-16.33% carbon dioxide, 1.4%-2.47% methane and 53.33-59.67% nitrogen.

Adnan *et al.* (2002) studied hydrogen production from sewage sludge by applying downdraft gasification technique. They conducted the experiment using a pilot scale throated downdraft gasifier and concluded that the combustible gases from sewage sludge had a high percentage of hydrogen



(8.98% to 11.4%) within 20.09% – 23.83% of combustible gases. This amount of gases is enough to run internal combustion engine.

Uma *et al.* (2004) reported that biomass gasification was one such process where producer gas could be obtained and used for power generation purposes. Biomass gasifier-based systems capable of producing power from a few kilowatts up to several hundred kilowatts had been successfully developed. They investigated emission characteristics of a diesel engine using diesel alone and producer gas which were used to run the diesel engine at different load conditions. The producer gas was produced by a downdraft gasifier system. The gas composition containing 14% hydrogen, 19% carbon monoxide, 10% carbon dioxide, 1.9% methane, and the remaining is nitrogen. Carbon monoxide emissions from the producer gas were higher than that from diesel alone at all operated load conditions, but nitrogen oxide and sulphur dioxide emissions decreased.

Based on studies reviewed, the maximum combustible gas composition obtained from producer gas produced through biomass gasification stated by the researchers has only below 24% by volume. Table 2.1 shows a summary of the producer gas composition obtained by other researchers in their experiments using downdraft gasifier.

**Table 2.1:** Gas composition in the producer gas reported by other researchers using downdraft gasifier.

	Biomass	% Vol.				
	Material	H <sub>2</sub>	CO	CO <sub>2</sub>	CH <sub>4</sub>	N <sub>2</sub>
Munoz et al. (2000)	wood residues	14	22	13	3	48
Sridhar et al. (2001)	causurina wood	19	19	12	2	48
Zainal et al. (2002)	furniture wood and wood chips	15	24	15	2	44
Dogru et al. (2002)	hazelnut shells	15	19	16	2	48
Uma et al. (2004)	saw dust of wood	14	19	10	2	55

To increase the percentage of combustible composition in the producer gas, some methods have to be studied. The hard work of other researchers to increase combustible composition in the producer gas is elaborated in Section 2.3.

### 2.2.6 Producer Gas Energy Content

Producer gas which is has the energy content greater than 4 MJ/Nm<sup>3</sup> can be applied to run a diesel engine (Kumar, 2010). The energy content of producer gas can be calculated from the energy content of the components using low and high heating values for each gas as shown in Equation 2.3.

$$HV_{pg} = \sum (\%vol.)_g (HV)_g \quad (2.3)$$